23rd ABCM International Congress of Mechanical Engineering
December 6-11, 2015, Rio de Janeiro, RJ, Brazil

AN ASSESSMENT OF CONVENTIONAL RANS TURBULENCE MODELS TO RESOLVE THE AIRFLOW OVER AIRCRAFT ENGINE INLETS AT HIGH ANGLES OF ATTACK

Leonardo Costa Almeida
Escola Politécnica da Universidade de São Paulo, Departamento de Engenharia Mecânica, São Paulo – SP – Brazil.
lcallmeida@gmail.com

Bruno Souza Carmo
Escola Politécnica da Universidade de São Paulo, Departamento de Engenharia Mecânica, São Paulo – SP – Brazil.
bruno.carmo@usp.br

Luis Gustavo Trapp
EMBRAER – Empresa Brasileira de Aeronáutica S.A., São José dos Campos – SP – Brazil.
gustavo.trapp@embraer.com.br

Abstract. *The flow over nacelle inlets plays a crucial role in the correct operation of the aircraft. One of the main issues regarding engine inlets is the flow separation which can occur at high angle-of-attack operations. Inlet distortion arises from these conditions and can cause fan and compressor instabilities, reducing the amount of thrust generated by the engine and compromising overall aircraft efficiency and performance. Compressor surge and stall can also occur along with structural issues due to eventual blade resonance, increasing values of actual stress and reducing fatigue life. Due to safety reasons, it is crucial to be able to accurately predict the performance of the engine throughout the aircraft operating envelope. This paper presents an investigation of numerical methodologies to simulate using computational fluid dynamics the flow over subsonic engine inlets operating at takeoff conditions, featured by low freestream Mach numbers and high angles of attack. Steady three-dimensional Reynolds-Averaged Navier-Stokes equations were solved using the commercial code CFD++. Three different turbulence models (Realizable k-epsilon, Spalart-Allmaras and k-omega SST) were assessed as to their capability to evaluate important flow features. For each model, results show distortion levels at the fan face, pressure recovery, pressure distribution along the lip, peak surface Mach number and separation angle. The numerical investigation was supported by previous wind tunnel test data performed on a long-duct nacelle of a commercial aircraft.*

Keywords: *nacelle, separation, distortion, CFD*

1. INTRODUCTION

This work aims to evaluate how well traditional RANS turbulence models resolve the flow around aircraft engine inlets operating at high angles of attack (AoA) conditions. Engine inlets perform in a variety of contrasting conditions such as takeoff and cruise and have to be capable of providing air to the engine in all these conditions in the most efficient way.

Non-uniformities of the airflow directed to the engine, also known as intake distortion, are largely amplified by the phenomenon of separation which can take place at the nacelle's lip at critical operating conditions, leading to loss of fan and compressor performance. Critical conditions include maximum power and high angles of attack during takeoff and occurrence of crosswind. Due to safety reasons, it is crucial to be able to accurately predict the performance of the engine throughout the operating envelope of the aircraft.

Experimental flight and wind tunnel testing are very expensive and therefore the use of computational fluid dynamics (CFD) tools has been increasing in industry. This works intends to show that the flow in and around a subsonic nacelle under high angles of attack in conditions typical of takeoff is very complex and difficult to predict by conventional turbulence models.

2. PHENOMENOLOGY

The pressure distribution at the nacelle's lip shows well-defined characteristics in some separation cases, being easily measured in-flight by pitot tubes. Many authors investigated the separation phenomenon by means of wind tunnel testing, but little has been done using computational tools. Luidens and Abbot (1976) performed wind tunnel runs at low Mach numbers in order to verify the separation phenomenon that can take place at inlets of STOL aircraft nacelles. By monitoring a specific static-pressure probe (located on the lip at about 20% of the axial throat length from the highlight) and a specific total-pressure probe at the diffuser-exit (located at about 80% of the hub-to-tip length), the authors were able to observe that, with the increase of the angle of attack of the nacelle, a continuous decrease in the lip static pressure occurred up to the separation angle, at which the pressure stopped to decrease and suddenly increased in value. At the diffuser-exit, total pressure would slightly decrease due to thickening of boundary layer up to the separation angle, at which a large decrease in value occurs.

Extensively used by engine manufacturers to stablish limits of correct operation for its engines, distortions coefficients also represent a good parameter to indicate inlet separation and provide a quantitative measurement of the flow quality directed to the core. The DC60 distortion coefficient is calculated by means of the Eq. (1):

$$DC60 = \frac{\min_{n} \bar{p}_{t,60} - \bar{p}_t}{\bar{p}_d} \quad (1)$$

in which $\bar{p}_{t,60}$ is the area-average total pressure in a 60° fan face circular sector, $\bar{p}_t$ is the area-average total pressure at the fan face and $\bar{p}_d$ is the area-average fan face dynamic pressure.

3. RESULTS AND DISCUSSION

This section provides the results obtained from simulations using CFD of the flow around inlets of aircraft engine nacelles operating at high angles of attack conditions. The results were compared to wind tunnel measurements. Three turbulence models usually used when performing RANS simulations were assessed: the realizable k-ε 2-equation model (Rke), the corrected version of Spalart-Allmaras 1-equation model (with curvature correction and inclusion of quadratic constitutive relation, SAcc) and Menter's k-ω SST model.

On previous investigation, a small-scale long-duct nacelle model of a commercial aircraft with spinner included was tested in wind tunnel in order to determine its flight envelope operating at high angles of attack. An ejector was responsible to pull the air from around into the nacelle, being able to reproduce real takeoff conditions (high mass flow rate per unity area). Instrumentation consisted of static pressure probes distributed along the inlet walls in different circumferential positions (shown in Figure 1) and of total pressure rakes at the fan face.

RANS – Reynolds Averaged Navier-Stokes Equations – equations were solved in its full, compressible and tridimensional form by the commercial code CFD++ from Metacomp Technologies, Inc.

Boundary conditions were:

- Pressure-farfield: semi-spherical domain, standard sea level conditions. The Mach number was 0.34 and angles were incremented from 10 to 30° in intervals of 1°.
- Pressure-outlet with mass flux imposition of $\dot{m}/A_{th} = 111.6\ kg/(s \cdot m^2)$, where A_{th} is the throat area of the nacelle.
- Symmetry plan with respect to the zero-yaw angle.

A fully-structured hexahedral mesh with approximately 4 million elements was built using the commercial package ANSYS ICEM v14.5. Y+ values were below 1 in all simulations performed. Figure 1 shows the mesh topology and boundary layer details at the symmetry plan.

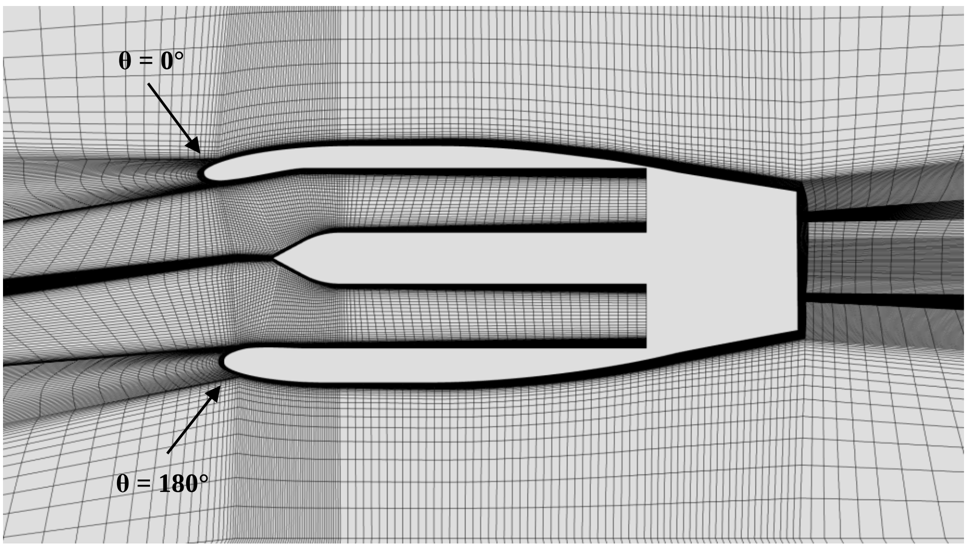

Figure 1. Mesh topology at the symmetry plan

It is important to highlight that the instrumentation and wind tunnel supports and walls were not included in the simulations, nor was the ejector. In its place, an outlet surface was included to play the role of the core. This surface was axially moved downstream of the lip in order to prevent any recirculating flow which could be present in cases were the flow separates, which was successfully achieved.

Figures 2 to 5 and Fig. 7 show the distribution of static pressure normalized by the freestream total pressure. Inlet axial station coordinates were normalized by the inlet axial length (L), such that 0 refers to the highlight and 1 to the fan face (coincident to the diffuser-exit). Due to disclosure of proprietary information, vertical-axis values were omitted.

At low angles of attack all turbulence models investigated showed similar results so that curves practically coincided. For this reason, initial investigations regarding sensibility analysis and the possibility of occurrence of blockage effects were performed using the SST model without loss of generality.

Figure 2 shows the pressure distribution at the lip at AoA = 0° and at the position θ = 180°.

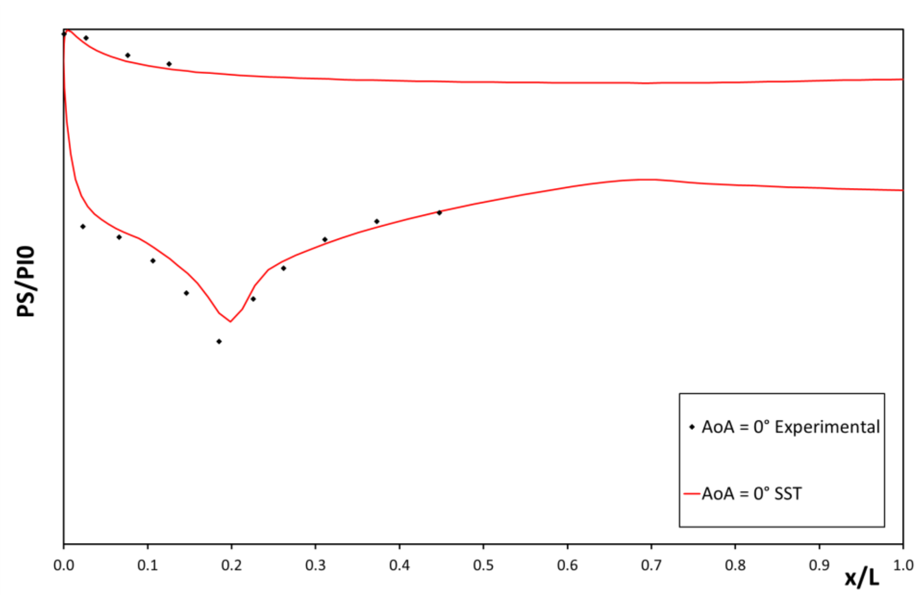

Figure 2. Pressure distribution at the lip at AoA = 0° and θ = 180° position

There is a good agreement between the CFD results and the tunnel measurements, especially at the external walls. In the internal walls there is a small difference at the stations between 0 and 0.2, namely, at the lip. It can be seen that the suction peak has been underestimated. This fact justified a sensibility analysis with respect to the mass flow rate value imposed at the outlet boundary condition. Figure 3 shows the results for zero angle of attack.

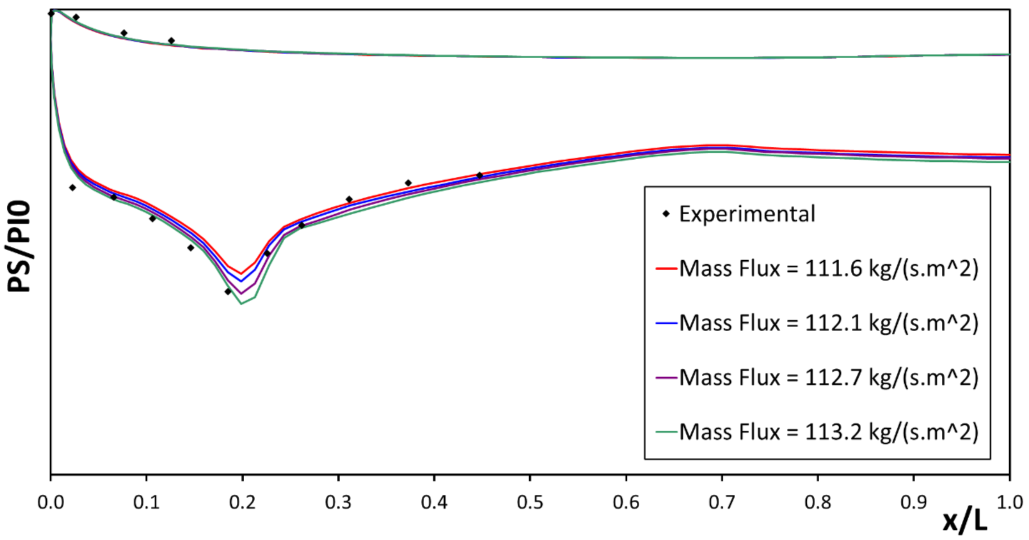

Figure 3. Sensibility analysis with respect to mass flux values at AoA = 0°

It can be seen that the suction peak corresponding to the mass flux rate of $112.7\ kg/(s \cdot m^2)$ closely agrees to the measurements. In order to verify if this close agreement would stand to higher angles, an angle of attack sweep was performed. The results are compared at AoA = 17° in Figure 4.

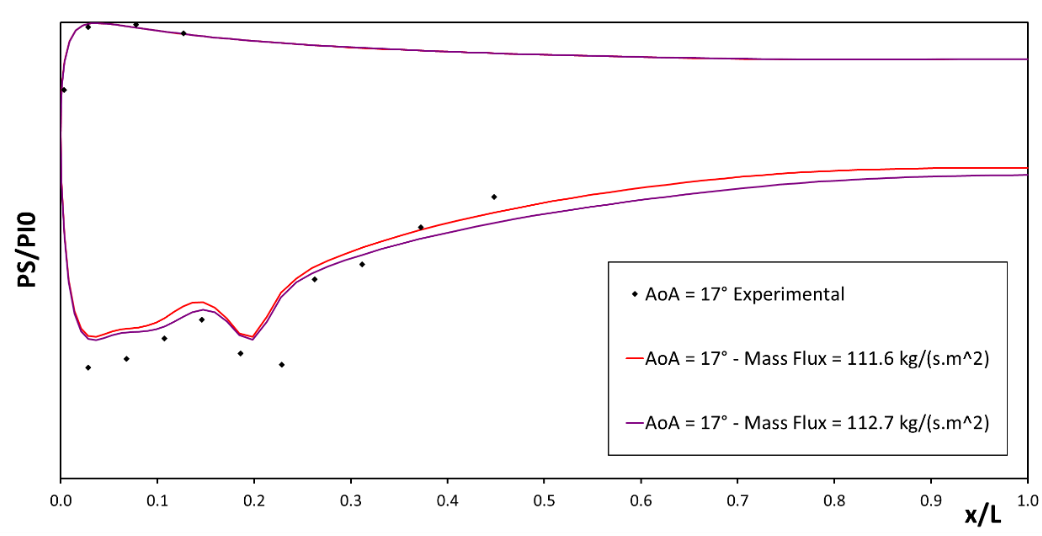

Figure 4. Comparison of pressure distribution between two different mass flux values

The suction peak did not increase with a higher mass flux, providing similar results to the original value. Not only that, downstream of the lip this higher mass flux leads pressure values to go away from the experimental values, suggesting that the $112.7\ kg/(s \cdot m^2)$ is indeed higher than the actual value used in tunnel.

Another aspect that had to be checked to confirm consistency between the testing and the simulations was the possibility of blockage effects that could have occurred in tunnel, once the simulations were performed considering an open domain, i.e. with the absence of tunnel walls and supports. If so, an angle of attack correction would be required in order to compare measurements to simulations in free-flight conditions. On a previous investigation of Trapp and Almeida (2014), it was found that the absence of tunnels walls, supports and instrumentation did not contribute to jeopardize the results.

Once it was concluded that the simulation setup was consistent with the wind tunnel testing, an assessment of how well the three turbulent models predict the flow at high angles of attack was done.

Figure 5 compares the pressure distribution at the lip at AoA = 10° and at the position θ = 180°.

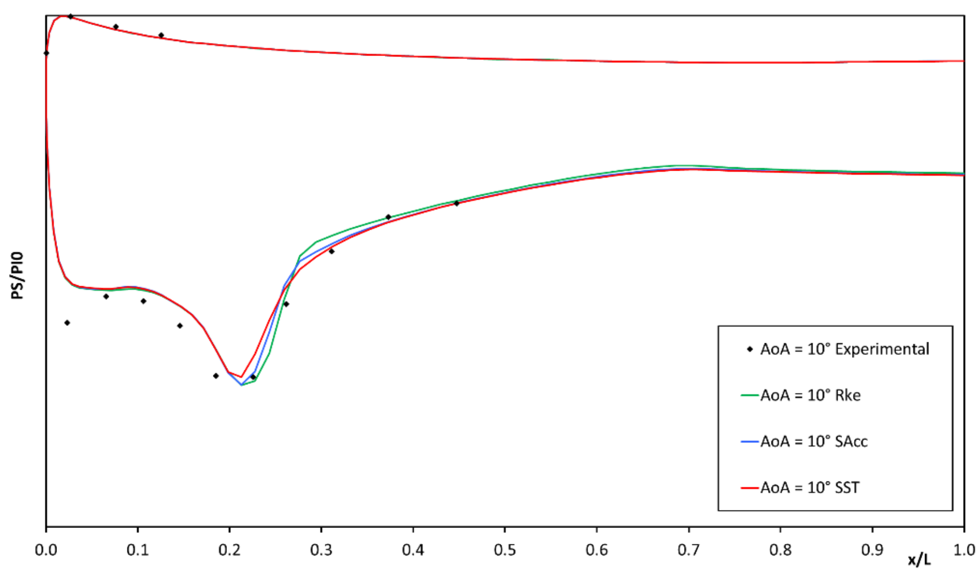

Figure 5. Pressure distribution at the lip at AoA = 10° and θ =180° position

There is a good agreement between CFD results and the measurements for all three turbulence models. However, once again there is a certain difficulty to correctly predict the intensity of the first suction peak.

Figure 6 shows contours of isentropic Mach number and surface streamlines at 10°, revealing a narrow separation which takes places near the throat. This narrow format is typical of separation induced by shock-boundary layer interaction due to the occurrence of locally supersonic regions at the lip, as pointed out by Probst, *et al*. (2012).

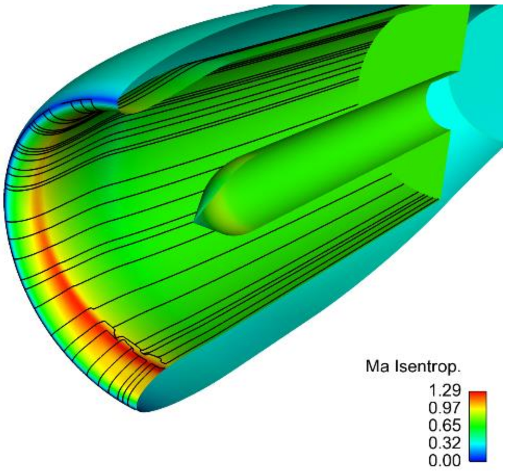

Figure 6. Contours of isentropic Mach number and surface streamlines at AoA = 10°

Figure 7 shows the evolution of the pressure distribution at the θ = 180° position with the increase of the angle of attack. As the separated region increases with the increase in angle of attack, a greater difference between CFD results and tunnel measurements is observed.

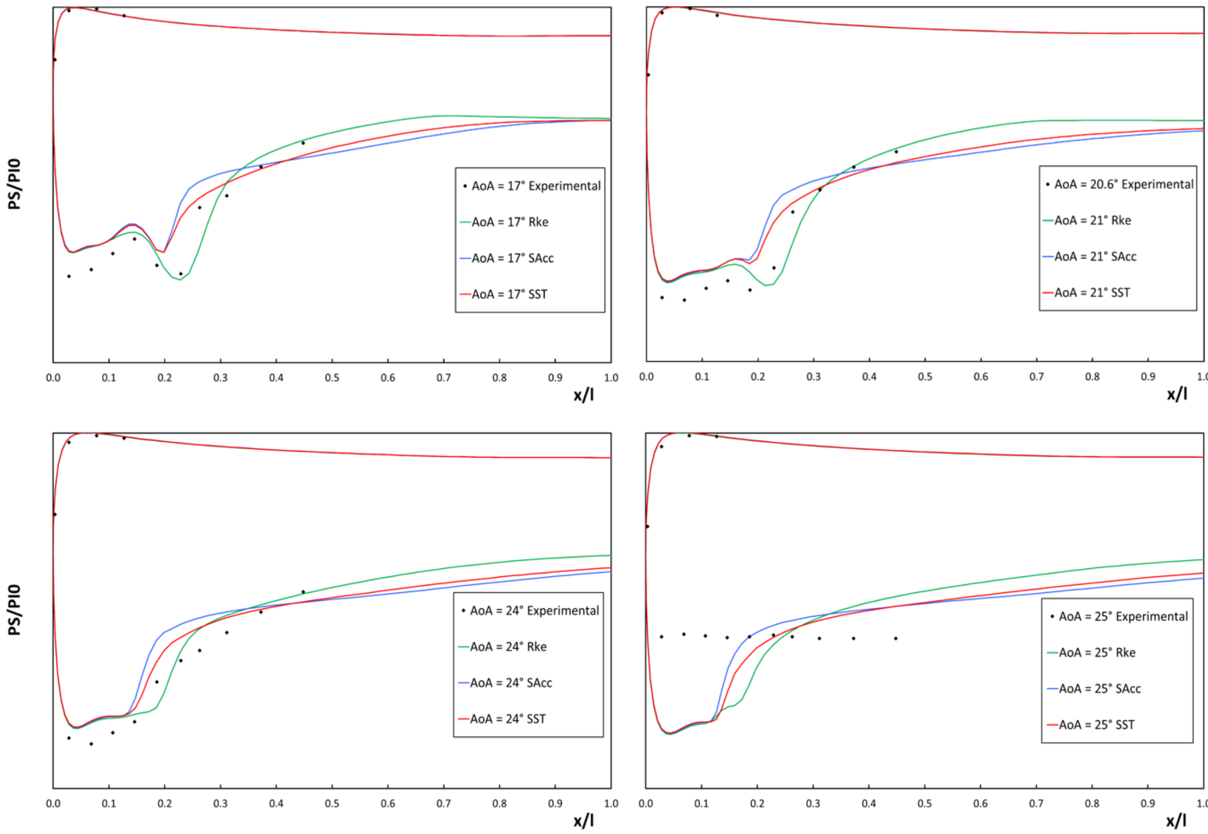

Figure 7. Pressure distribution at the lip at θ = 180° position

At AoA = 25° the flow in the tunnel testing collapsed, which is shown by the complete horizontal aspect of the pressure curve. This boundary layer collapse is physically shown by a sudden movement of the separation line to the leading-edge (highlight) of the nacelle as shown in Figure 8 for the SST model.

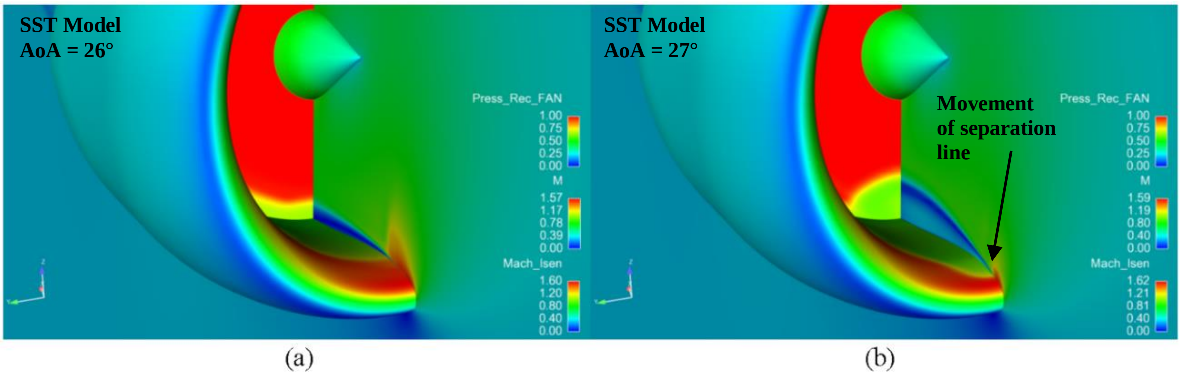

Figure 8. Boundary layer collapse and movement of the separation line onto the leading-edge

This sudden movement of the separated region can be observed in the distortion coefficient curve as a great increase in the distortion value, which is clearly shown by the experimental curve in Figure 9.

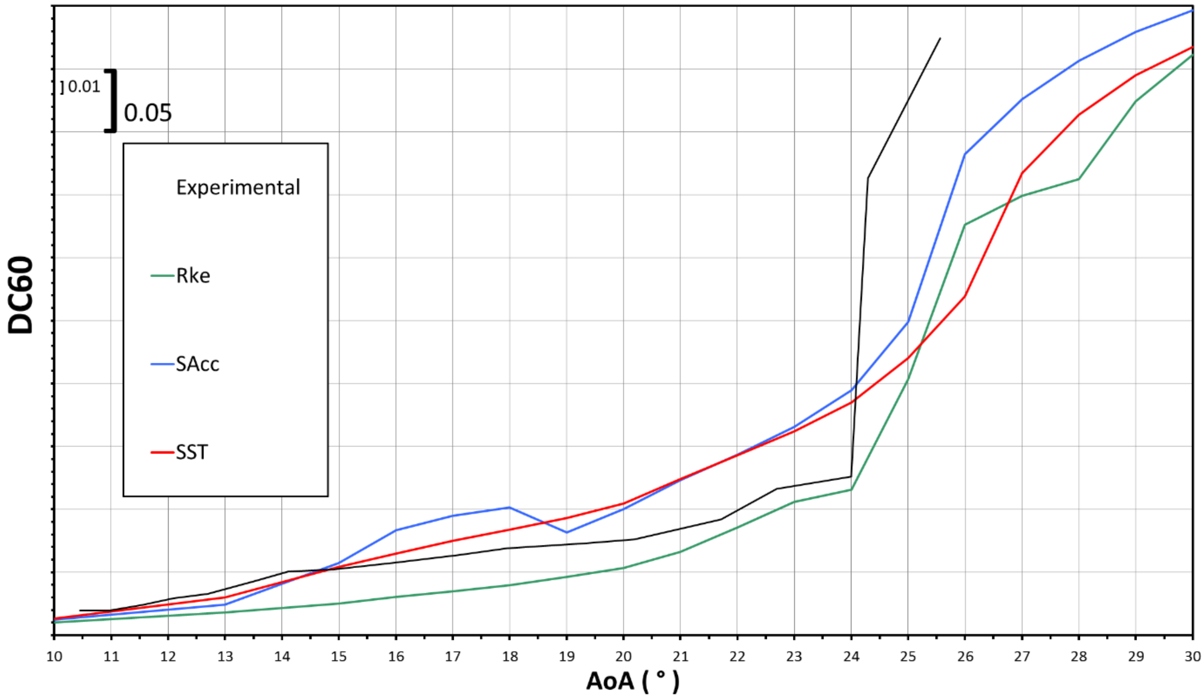

Figure 9. Comparison of DC60 distortion coefficients predicted by the three turbulence models

All turbulence models overpredicted the leading-edge separation angle. The k-ε and Spallart Almaras models indicated 26°, while k-ω SST indicated 27°. This overprediction of a massive separation angle is consistent with the pressure measurements, once a higher static pressure means a lower value of isentropic Mach number. In cases of maximum power and high mass flux to the engine, flow separation is induced by peak values of Mach number (Luidens and Abbot, 1976), which explains the overprediction of the angle at which the collapse occurs.

4. CONCLUSION

In the present work, an investigation of conventional turbulence models was conducted in order to assess their capability of predicting flow separation which might take place at nacelle inlets operating under high angles of attack. Steady CFD simulations exhibit good representativeness of the flow and in general agree well with measurements. However, these conventional turbulence models show difficulties to accurately predict the intensity of the suction peak, which takes place at the inlet lip. According to Probst, *et al*. (2012), at conditions close to nacelle stall, the assumption of isotropic turbulence is not consistent, which partially explains the fact that conventional RANS models fail to accurately predict the suction peak and consequently the peak isentropic Mach number values, hence delaying separation. On the other hand, all models provide reasonable results in terms of distortion levels at low angles of attack, prior to leading-edge separation. The k-ω SST model provided closer values and has the tendency to overestimate distortion levels, thus providing conservatism in a preliminary design of engine inlets. In order to better resolve the complex phenomena of separation occurring at the inlet of aircraft nacelles, more reliable turbulence models and methodologies have to be investigated.

5. ACKNOWLEDGEMENTS

The authors would like to thank the support given by EMBRAER.

6. REFERENCES

Anderson, B. H., Baust, H. D., and Agrell, J., 2002. “Management of Total Pressure Recovery, Distortion and High Cycle Fatigue in Compact Air Vehicle Inlets”. NASA TM-212000.

Boles, M. A., Luidens, R. W., and Stockman, N. O., 1978. “Theoretical Flow Characteristics of Inlets for Tilting-Nacelle VTOL Aircraft”. NASA TP-1205 c.1.

Chou, D. C., Luidens, R. W. and Stockman, N. O., 1977. “Prediction of Laminar and Turbulent Boundary Layer Flow Separation in V/STOL Engine Inlets”. NASA TMX-73575.

Luidens, R. W. and Abbot, J. M., 1976. “Incidence Angle Bounds for Lip Flow Separation of three 13.97-centimeter-diameter Inlets”. NASA TMX-3351.

Probst, A., Schulze, S., Kahler, C.J. and Radespiel, R., 2012. “Reynolds Stress Modelling of Subsonic and Transonic Inlet Stall Compared to Measurements”. Third Symposium of Wing and Nacelle Stall, Braunschweig, www.for1066.tu-bs.de.

Trapp, L. G., 2012. "Flow Analysis of an Engine Nacelle in Crosswind: Inlet Vortices and their Interactions". Ph.D. thesis in Aeronautics and Mechanical Engineering, Instituto Tecnológico da Aeronáutica. São José dos Campos, Brazil.

Trapp, L. G. and Almeida, L. C., 2014. “Validation of RANS Numerical Methodologies to Simulate Nacelles at High Angles of Attack using CFD”. Embraer S.A., São José dos Campos, Brazil.

7. RESPONSIBILITY NOTICE